

## Inverting a Supernova: Neutrino Mixing, Temperatures and Binding Energy

<sup>1</sup>V. Barger, <sup>2</sup>D. Marfatia and <sup>1</sup>B. P. Wood

<sup>1</sup>Department of Physics, University of Wisconsin, Madison, WI 53706

<sup>2</sup>Department of Physics, Boston University, Boston, MA 02215

We show that the mixing angle  $\theta_{13}$ , the temperatures of the emergent neutrinos and the binding energy released by a galactic Type II supernova are determinable (assuming the LMA solution is correct) from observations at the Sudbury Neutrino Observatory (SNO) and at Super-Kamiokande (SK). We implement a supernova-model-independent analysis of the neutronization burst events at SNO that could yield stringent bounds on  $\sin^2 2\theta_{13}$  if the neutrino mass hierarchy is normal. We demonstrate that a combined analysis of the SNO and SK events will provide a precise determination of the temperatures of the non-electron neutrinos and the binding energy of the supernova and will place bounds on  $\sin^2 2\theta_{13}$  irrespective of whether the mass hierarchy is normal or inverted.

Neutrino oscillations convincingly explain the solar and atmospheric neutrino anomalies [1,2]. Atmospheric data and initial K2K data [3] indicate oscillations with  $\Delta m_{31}^2 \approx 3 \times 10^3 \text{ eV}^2$  and  $\sin^2 2\theta_{23} \approx 1$  [4], that will be tested to within 10% accuracy at MINOS [5,6]. The large mixing angle (LMA) solution ( $\Delta m_{21}^2 \approx 5 \times 10^5 \text{ eV}^2$ ,  $\sin^2 2\theta_{12} \approx 0.8$ ) which is emerging as the solution to the solar neutrino problem [7] will be tested to 10% accuracy [8] at KamLAND [9]. Thus, in the near future, all parameters relevant to neutrino oscillations will be known, except  $\sin^2 2\theta_{13}$ , which is bounded above by 0.1 at the 95% C.L. by the CHOOZ experiment [10], and the sign of  $\Delta m_{31}^2$ .

The objective of this Letter is to determine what the expected neutrino signals at SNO and SK (after its re-instrumentation) from a Type II galactic supernova can tell us about  $\sin^2 2\theta_{13}$ ,  $\text{sgn}(\Delta m_{31}^2)$ , the neutrino temperatures, and the binding energy released in such an event if the LMA solution is confirmed. Throughout, we assume that solar and atmospheric parameters will be known to within 10% from upcoming experiments. Since low energy  $\bar{\nu}_e$  and  $\nu_e$  are indistinguishable at SNO and SK, only their transitions with  $\nu_e$  can be studied.

Supernova neutrinos: During the early stages of a supernova explosion, as the shock wave rebounds from the dense inner core of the star and crosses the electron neutrinosphere,  $\bar{\nu}_e$ 's from electron capture on protons are released resulting in a breakout or neutronization burst that carries away  $10^{51}$  ergs. The duration of this burst lasts only a few milliseconds (no more than 10) and any non-electron neutrino events at SNO during this time are a consequence of  $\bar{\nu}_e$  oscillations. For progenitor stars of mass  $15M_\odot$ , numerical simulations find that

following the neutronization burst, 99% of the binding energy released,  $E_b = 1.5 - 4.5 \times 10^{53}$  ergs, is equipartitioned in the form of neutrinos and antineutrinos of all flavors. This occurs on a timescale of tens of seconds. The mean temperatures of the different flavors of neutrinos are determined by the strength of their interactions with matter, with the most strongly interacting neutrinos leaving the star with the lowest temperature. Then,  $\mu_{\nu_e} = 2\mu_{\nu_\mu}$  and  $\mu_{\nu_\tau} = 3\mu_{\nu_e}$  with  $\mu_{\nu_e} \approx 5 \text{ MeV}$  and  $x = \mu_{\nu_\mu}/\mu_{\nu_e} = \mu_{\nu_\tau}/\mu_{\nu_e}$ . The distributions of the neutrinos are Fermi-Dirac aside from pinching of the distributions during the cooling phase whose effects are insignificant in the time-averaged spectra.

As the neutrinos leave the star, they encounter a density profile that falls like  $1=r^{-3}$  [11]. If the mass hierarchy is normal, i.e.  $\Delta m_{31}^2 > 0$ , (inverted, i.e.  $\Delta m_{31}^2 < 0$ ), neutrinos (antineutrinos) pass through a resonance at high densities ( $10^3 - 10^4 \text{ g/cm}^3$ ) which is characterized by  $(\Delta m_{31}^2; \sin^2 2\theta_{13})$  and the neutrinos pass through a second resonance at low densities ( $\approx 20 \text{ g/cm}^3$  for the LMA solution) that is determined by  $(\Delta m_{21}^2; \sin^2 2\theta_{12})$  [12]. Transitions in the latter resonance are almost adiabatic, with a zero probability of level crossing. We denote the jumping probability in the high density resonance by  $P_H$  and adopt a potential that gives the same  $P_H$  as in Fig. 2 of Ref. [13]. Note that  $P_H$  is the same for both neutrinos and antineutrinos [13] and has an  $e^{-\sin^2 \theta_{13} (\Delta m_{31}^2/E)^2}$  dependence [14].

The neutronization burst and SNO: To simulate the pulse-like nature of the neutronization burst spectrum, we use a pinched Fermi-Dirac spectrum with pinching parameter  $\alpha = 11$  as in Ref. [15]. We assume only lim-

ited knowledge of the average energy of the neutrinos,  $\langle E_{\text{nb}} \rangle$ , and no knowledge of the total energy released in the burst.

For the inverted hierarchy, the survival probability  $P = P_{2e}$  [12], which is the probability that a neutrino reaching the earth in the  $\nu_2$  mass eigenstate will interact in a detector as  $\nu_e$ . Since  $P_{2e}$  depends only on oscillation parameters at the solar scale, nothing can be learned about  $\sin^2 2_{13}$  from the neutronization burst if the hierarchy is inverted.

We therefore turn to the normal hierarchy, for which the flux from the burst will be partially or completely converted into  $\nu_e$  and with the survival probability given by [12]

$$P = P_H P_{2e} + (1 - P_H) \sin^2 2_{13} : \quad (1)$$

Now, the sensitivity of the signal depends on  $\sin^2 2_{13}$  both explicitly and implicitly through  $P_H$ .

The neutrinos will mainly interact with deuterium in the 1 kton fiducial volume of the heavy water tank (with a 5 MeV threshold) at SNO via the charged current (CC) and neutral current (NC) reactions,

$$\nu_e + d \rightarrow p + p + e^- ; \quad (2)$$

$$\nu_e + d \rightarrow \nu_y + p + n ; \quad \nu_y = \nu_e ; \quad (3)$$

The number of NC events is indicative of the total  $\nu_e$  flux leaving the star and the number of CC events reflects the flux of surviving  $\nu_e$ . Together they provide a measure of the survival probability in Eq. (1) and therefore of  $\sin^2 2_{13}$  assuming  $m_{31}^2$  and the solar parameters are already precisely measured.

We consider possible numbers of CC and NC events that could be realized at SNO for a supernova at a distance of 10 kpc which is slightly greater than the distance to the center of our galaxy (8.5 kpc). For each pair of possible numbers,  $N_{CC}$  and  $N_{NC}$ , we consider the ratio  $N_{CC}/(N_{CC} + N_{NC})$  which is independent of both the energy released in the burst and the distance to the star, and is only weakly dependent on the average energy of the neutrinos. Our choice of 10 kpc for the star's distance simply sets the scale for the number of events that can be expected at the SNO detector. To calculate  $N_{CC}$  and  $N_{NC}$ , we assume that SNO is operating with its  $^3\text{He}$  Neutral Current Detectors giving a neutron capture efficiency of 57% [16]. We also assume that since the time delay for neutron capture is sharply peaked at 16 ms, it will be possible to correct the timing information of the NC events to ensure that they occurred during the neutronization burst. We determine the bounds that can be placed on  $\sin^2 2_{13}$  for each pair of possible rates. The upper or lower bounds are found by optimizing the ratio  $N_{CC}^{\text{th}} = (N_{CC}^{\text{th}} + N_{NC}^{\text{th}})$  with respect to  $\sin^2 2_{12}$ ,  $m_{21}^2$ ,  $m_{31}^2$ ,  $\langle E_{\text{nb}} \rangle$  and the supernova zenith angle so as to give the most conservative bounds on  $\sin^2 2_{13}$ . The solar

N <sub>CC</sub>	N <sub>NC</sub>	Upper Bound		Lower Bound			
		90%	95%	90%	95%		
1	2						
2	2	4:3	10 <sup>-4</sup>	5:1	10 <sup>-4</sup>		
3	2	2:9	10 <sup>-4</sup>	3:6	10 <sup>-4</sup>		
1	3						
2	3	4:8	10 <sup>-4</sup>				
3	3	3:4	10 <sup>-4</sup>	4:1	10 <sup>-4</sup>		
4	3	2:6	10 <sup>-4</sup>	3:2	10 <sup>-4</sup>		
0	4					2:5	10 <sup>-5</sup>
1	4						
2	4	5:2	10 <sup>-4</sup>				
3	4	3:8	10 <sup>-4</sup>	4:5	10 <sup>-4</sup>		
4	4	3:0	10 <sup>-4</sup>	3:5	10 <sup>-4</sup>		
5	4	2:4	10 <sup>-4</sup>	2:9	10 <sup>-4</sup>		
0	5					4:8	10 <sup>-5</sup>
1	5						
2	5						
3	5	4:2	10 <sup>-4</sup>	4:8	10 <sup>-4</sup>		
4	5	3:3	10 <sup>-4</sup>	3:9	10 <sup>-4</sup>		
5	5	2:7	10 <sup>-4</sup>	3:2	10 <sup>-4</sup>		
6	5	2:2	10 <sup>-4</sup>	2:7	10 <sup>-4</sup>		
0	6					6:7	10 <sup>-5</sup>
0	7					8:4	10 <sup>-5</sup>
0	10					1:2	10 <sup>-4</sup>
						4:0	10 <sup>-5</sup>
						5:6	10 <sup>-5</sup>
						9:3	10 <sup>-5</sup>

TABLE 1: Bounds obtainable on  $\sin^2 2_{13}$  from the CC and NC events at SNO associated with the neutronization burst.

parameters are varied by 10% around their central values  $\sin^2 2_{12} = 0.79$  and  $m_{21}^2 = 3.7 \cdot 10^5 \text{ eV}^2$  in anticipation of KamLAND's sensitivity [8],  $m_{31}^2$  is varied within its projected 90% C.L. range as given by the combination of SK atmospheric data and K2K data with error bars halved [4] (as very conservatively expected from the MINOS experiment [5,6]), and  $\langle E_{\text{nb}} \rangle$  is allowed to take values between 10 and 20 MeV.

The bounds in Table 1 are the single-sided confidence limits for binomial statistics, appropriate since ratios of small numbers are involved [17]. For many possible data pairs, SNO will be able to place a 95% C.L. upper bound on  $\sin^2 2_{13}$  that is more than two orders of magnitude below its current value. If no CC events and a large number of NC events are observed, lower bounds on  $\sin^2 2_{13}$  can be placed because this occurs for  $P_H = 0$  which implies a relatively large  $\sin^2 2_{13}$ . A side from the fact that the NC cross-section and efficiency are smaller than those for the CC reaction, the situation in which the  $N_{CC}$  is significantly larger than  $N_{NC}$  will be the result of a statistical fluctuation and we do not consider it.

The integrated spectra at SNO and SK: Information on the neutrinos emerging from the supernova after the neutronization burst will be contained in  $\nu_e$  and  $\bar{\nu}_e$  spectra observed at SNO and SK.

For the normal hierarchy, the survival probability for electron anti-neutrinos is  $P = P_{1e}$  [12], which is the probability that an antineutrino reaching the earth in the  $\nu_1$  mass eigenstate interacts as a  $\nu_e$ . For the inverted hierarchy, we have  $P = P_H P_{1e} + (1 - P_H) \sin^2 2_{13}$  [12]. Thus,

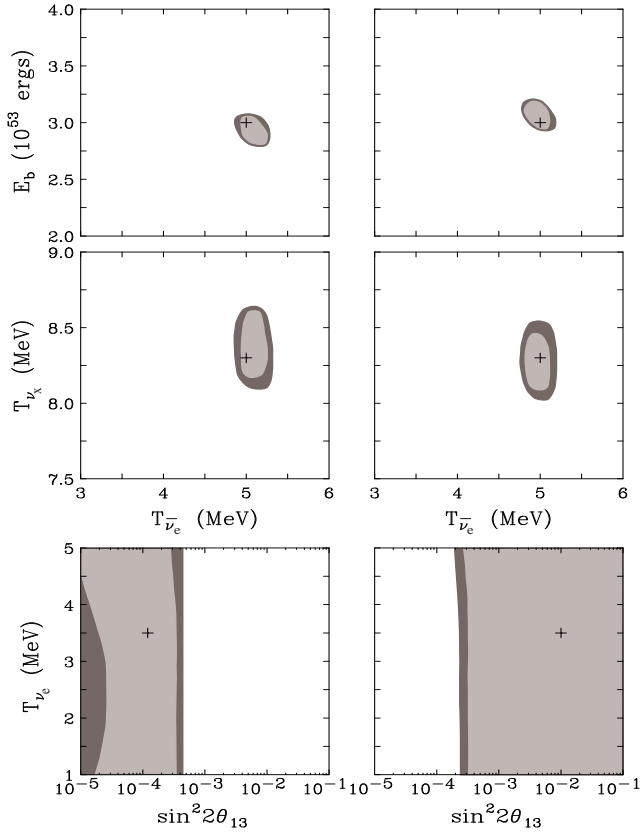


FIG. 1. Determination of  $\sin^2 2\theta_{13}$ , the binding energy  $E_b$ , and the supernova neutrino temperatures for the normal mass hierarchy. The left-hand panels correspond to data simulated at  $\sin^2 2\theta_{13} = 1.2 \cdot 10^{-4}$ . The right-hand panels correspond to data simulated at  $\sin^2 2\theta_{13} = 10^{-2}$  ( $P_H = 0$ ). The cross-hairs mark the theoretical inputs, and the 90% and 99% C.L. regions are light and dark shadings, respectively.  $T_x$  is the temperature of the non-electron neutrinos.

the  $\nu_e$  spectrum will be more sensitive to  $\sin^2 2\theta_{13}$  if the hierarchy is inverted.

For the 32 kton ductial volume of the SK detector (with a 7.5 MeV threshold), and the 1.4 kton ductial volume of the light water tank at SNO (with a threshold of 5 MeV), we only consider events that are isotropic and indistinguishable from each other; they are

$$\nu_e + p \rightarrow n + e^+; \quad (4)$$

$$\nu_e + O \rightarrow F + e; \quad \nu_e + O \rightarrow N + e^+; \quad (5)$$

We do not consider electron scattering events. The good directional capability on these events allows their separation, and they play an important role in the reconstruction of the direction of the supernova that in turn determines the extent to which earth matter effects are important [18].

For the 1 kton heavy water tank at SNO, we include the  $\nu_e$  CC reaction,

$$\nu_e + d \rightarrow n + n + e^+; \quad (6)$$

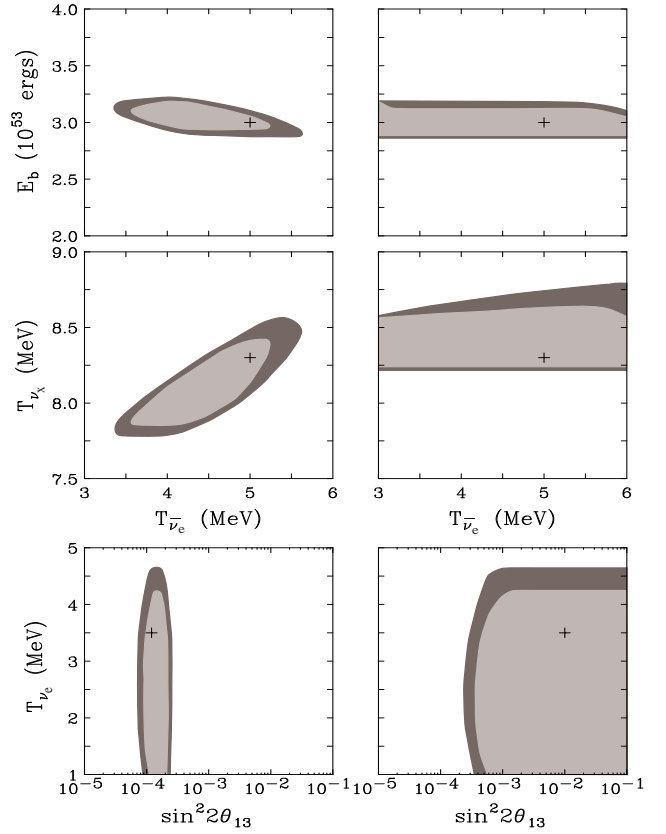


FIG. 2. The same as Fig. 1 but for an inverted hierarchy.

in addition to the processes (2) and (5). Two neutron captures in addition to a Cherenkov cone can distinguish these events from the other charged current scattering events on deuterium or oxygen. All NC events (whose signal is a single neutron capture and no electron), and electron scattering events are neglected.

To simulate the energy spectra for the channels under consideration at the two experiments we assume a typical supernova [15,20] at a distance of 10 kpc, with  $E_b = 3 \cdot 10^{53}$  ergs,  $T_{\nu_e} = 3.5$  MeV,  $T_{\nu_x} = 5$  MeV, and  $T_x = 8.3$  MeV. We set  $\sin^2 2\theta_{12} = 0.79$ ,  $m_{21}^2 = 3.7 \cdot 10^5$  eV<sup>2</sup> and  $|m_{31}^2| = 3 \cdot 10^3$  eV<sup>2</sup>, since variation of these parameters within their future bounds has very little effect on the analysis. In all, there are four spectra; one for SK, one for the light water tank at SNO, one for processes (2) and (5), and one for process (6). We simulate four datasets, two for each type of hierarchy and for two values of  $\sin^2 2\theta_{13}$  for which it is possible to distinguish between the two hierarchies; if  $\sin^2 2\theta_{13} < 10^{-4}$ ,  $\text{sgn}(m_{31}^2)$  is indeterminate [12,19]. We perform a  $\chi^2$  analysis, freely varying  $E_b$ ,  $T_{\nu_e}$ ,  $T_{\nu_x}$ ,  $T_x$ , and  $\sin^2 2\theta_{13}$  to find the best fit points and the 90% ( $\chi^2 < 9.24$ ) and 99% C.L. ( $\chi^2 < 15.1$ ) allowed regions.

Figure 1 shows the results of this fit for the normal hierarchy. The left-hand panels show the determination of the supernova parameters and  $\sin^2 2\theta_{13}$  for data sim-

ulated at  $\sin^2 2_{13} = 1.2 \cdot 10^{-4}$ . We see that all the supernova parameters except  $T_e$  can be determined with high precision by this combined analysis, and an upper bound can be placed at  $\sin^2 2_{13} = 4 \cdot 10^{-4}$  at the 99% C.L.. The right-hand panels of Fig. 1 show the results of the same analysis done with the data simulated at  $\sin^2 2_{13} = 10^{-2}$ , for which  $P_H = 0$ . The supernova parameters are determined with the same precision, and this time a lower bound is placed at  $\sin^2 2_{13} = 2 \cdot 10^{-4}$  at the 99% C.L.. For a wide range of  $m_{21}^2$ , we find that a 99% C.L. upper bound can be placed if  $\sin^2 2_{13} < 1.5 \cdot 10^{-4}$ , and a 99% C.L. lower bound can be placed if  $\sin^2 2_{13} > 4 \cdot 10^{-4}$ . For the small range of values in between, it may not be possible to place a bound at the 99% C.L. although 90% C.L. bounds can be placed. Since the overall normalization of the neutrino fluxes depends critically on  $E_b$ , it is determined with excellent accuracy. The values of  $T_e$  and  $T_x$  are also determined precisely since these parameters control the  $\nu_e$  spectral distortion (which is independent of  $\sin^2 2_{13}$ ) obtained from thousands of events at SK and hundreds more at SNO. Sensitivity to  $\sin^2 2_{13}$  is achieved via  $\nu_e$ -d events at SNO and  $\nu_e$ -O events at SK and SNO.

Figure 2 shows the results of the 5-parameter fit for the inverted hierarchy. A gain, the left-hand column corresponds to data simulated at  $\sin^2 2_{13} = 1.2 \cdot 10^{-4}$ . A small allowed region is obtained for  $\sin^2 2_{13}$  for two reasons: the  $\nu_e$  spectrum is more sensitive to  $\sin^2 2_{13}$  in the inverted hierarchy and the  $\nu_e$  signal at SK is huge. The right-hand column of Fig. 2 shows similar plots for data simulated with  $\sin^2 2_{13} = 10^{-2}$ . In this case (and for any  $\sin^2 2_{13}$  for which  $P_H = 0$ ),  $\sin^2 2_{13}$  and  $T_e$  cannot be simultaneously bounded if both are left free. When we restrict  $T_e$  to lie between 3 and 7 MeV, a lower bound of  $\sin^2 2_{13} = 2 \cdot 10^{-4}$  is obtained at the 99% C.L.. When data are simulated at  $\sin^2 2_{13} < 10^{-5}$  ( $> 2 \cdot 10^{-4}$ ), only an upper (lower) bound can be placed. In the inverted hierarchy, we have a lesser sensitivity to  $T_e$  and  $T_x$ , since the  $\nu_e$  flux is also sensitive to  $\sin^2 2_{13}$  leading to competition between these parameters.

Although the regions in Figs. 1 and 2 are calculated assuming that the neutrinos detected at SK crossed both the mantle and core of the earth, and those at SNO crossed the mantle only, we have established that the bounds placed are largely independent of the supernova's zenith angles at the two experiments.

If the hierarchy is unknown at the time of a supernova signal, it can be deduced if  $\sin^2 2_{13} > 10^{-4}$ . We have confirmed this to be the case by analyzing each dataset with both hierarchies and finding that only the hierarchy for which the dataset was simulated gives a good solution, while the other hierarchy is disfavored at more than 3 $\sigma$ . For  $\sin^2 2_{13} > 2 \cdot 10^{-4}$ , one hierarchy is a better fit than the other by more than 5 $\sigma$ . For values of  $\sin^2 2_{13}$  smaller than  $10^{-4}$ ,  $P_H$  is not close to zero and the survival probabilities are similar for the two cases [12].

**Summary:** We have considered what information can be extracted from neutrinos detected at SNO and SK from a galactic supernova. If the neutrino mass hierarchy is normal, the neutronization burst alone can provide an upper bound ( $O(10^{-4})$ ) or lower bound ( $O(10^{-5})$ ) on  $\sin^2 2_{13}$  independently of supernova models and earth matter effects. The bulk of the neutrinos emerge after the burst. The information they carry is of importance in understanding the astrophysics of supernovae. The binding energy released in the supernova and the temperatures of the neutrinos expelled may be determined with considerable precision for most values of  $\sin^2 2_{13}$ . Furthermore, bounds on  $\sin^2 2_{13}$  can be placed irrespective of the mass hierarchy. If  $\sin^2 2_{13} > 10^{-4}$ , the hierarchy can be determined.

**Acknowledgments:** We thank E. Beier, E. Kearns, R. Robertson and C. Walter for discussions. This research was supported by the U.S. DOE under Grants No. DE-FG 02-95ER 40896 and No. DE-FG 02-91ER 40676 and by the W.A.R.F.

- 
- [1] B. Cleveland et al., *Astropart. Phys.* 496, 505 (1998); J. Abdurashitov et al., *Phys. Rev. C* 60, 055801 (1999); W. Hampel et al., *Phys. Lett. B* 447, 127 (1999); S. Fukuda et al., *Phys. Rev. Lett.* 86, 5656 (2001); Q. Ahmad et al., *Phys. Rev. Lett.* 87, 071301 (2001).
  - [2] Y. Fukuda et al., *Phys. Lett. B* 467, 185 (1999); W. Allison et al., *Phys. Lett. B* 449, 137 (1999); M. Ambrosio et al., hep-ex/0106049.
  - [3] S.H. Ahn et al., hep-ex/0103001.
  - [4] G.L. Fogli, E. Lisi and A. Marrone, hep-ph/01110089.
  - [5] Fermilab Report No. NuM I-L-375 (1998).
  - [6] V. Barger et al., hep-ph/0110393.
  - [7] V. Barger et al., hep-ph/0106207; J.N. Bahcall et al., hep-ph/0111150; G.L. Fogli et al., *Phys. Rev. D* 64, 093007 (2001); A. Bandyopadhyay et al., *Phys. Lett. B* 519, 83 (2001).
  - [8] V. Barger, D. Marfatia and B.P. Wood, *Phys. Lett. B* 498, 53 (2001).
  - [9] The KamLAND proposal, Stanford-HEP-98-03.
  - [10] M. Apollonio et al., *Phys. Lett. B* 466, 415 (1999).
  - [11] G. Brown, H. Bethe and G. Baym, *Nucl. Phys. A* 375, 481 (1982).
  - [12] A.S. Dighe and A.Yu. Smirnov, *Phys. Rev. D* 62, 033007 (2000).
  - [13] G.L. Fogli, et al., hep-ph/0111199.
  - [14] T.K. Kuo and J. Pantaleone, *Phys. Rev. D* 37 298 (1988).
  - [15] A. Burrows, D. Klein and R. Gandhi, *Phys. Rev. D* 60, 53003 (1991).
  - [16] C.J. Virtue, *Nucl. Phys. Proc. Suppl.* 100, 326 (2001).
  - [17] N. Gehrels, *Ap. J.* 303, 336 (1986).
  - [18] C. Lunardini and A.Yu. Smirnov, *Nucl. Phys. B* 616, 307 (2001).
  - [19] H. Minakata and H. Nunokawa, *Phys. Lett. B* 504, 301 (2001).
  - [20] H.E. Dalhed, J.R. Wilson and R.W. Mayle, *Nucl. Phys. Proc. Suppl.* 77, 429 (1999).